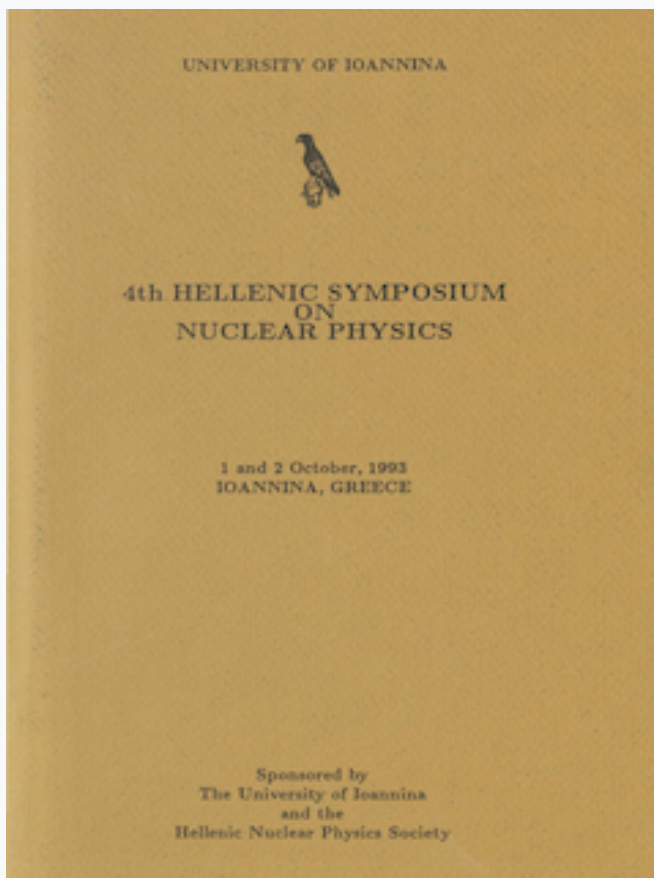


## HNPS Advances in Nuclear Physics

Vol 4 (1993)

HNPS1993



### Projectile Fragmentation of 16O and 32S beams from Dubna LHE Synchrotron

*D. Sampsonidis, B. A. Kulakov, M. I. Krivopustov, V. S. Butsev, M. Zamani*

doi: [10.12681/hnps.2882](https://doi.org/10.12681/hnps.2882)

#### To cite this article:

Sampsonidis, D., Kulakov, B. A., Krivopustov, M. I., Butsev, V. S., & Zamani, M. (2020). Projectile Fragmentation of 16O and 32S beams from Dubna LHE Synchrotron. *HNPS Advances in Nuclear Physics*, 4, 163–169. <https://doi.org/10.12681/hnps.2882>

## PROJECTILE FRAGMENTATION OF $^{16}\text{O}$ AND $^{32}\text{S}$ BEAMS FROM DUBNA LHE SYNCHROPHASOTRON

D.Sampsonidis<sup>1</sup>, B.A.Kulakov<sup>2</sup>, M.I.Krivopustov<sup>2</sup>, V.S.Butsev<sup>2</sup> and M.Zamani<sup>1</sup>.

<sup>1</sup> University of Thessaloniki, 540 06 Thessaloniki Greece

<sup>2</sup> Joint Institute for Nuclear Research, 141980 Dubna Russia

### Abstract

We investigate the charge changing collisions for  $^{16}\text{O}$  and  $^{32}\text{S}$  beams, using the experimental method of Solid State Nuclear Track Detectors (SSNTD). Sample reading was performed by an automatic measurement system. We determined the total charge changing cross sections and the partial cross sections for the production of fragments of charge  $9 \leq Z \leq 14$ .

### 1. Introduction

The total reaction cross-section ( $\sigma_{\text{tot}}$ ) as well as the partial reaction cross-section ( $\sigma_{\text{p}}$ ) in Heavy Ion Reactions at intermediate and high energies, carry significant information concerning the reaction. Both  $\sigma_{\text{tot}}$  and  $\sigma_{\text{p}}$ , compared to theoretical calculations according to several models, can lead to qualitative results which concern the reaction mechanism and the structure of the nucleus.

The fragments arising from the beam fragmentation, have the beam velocity (since the momentum transfer to the target is negligible) therefore, they can be identified using the relation charge -  $dE/dx$ . This is the property upon which the method for charge discrimination during the calculation of both  $\sigma_{\text{tot}}$  and  $\sigma_{\text{p}}$ , is based.

The detection of ionising particles using SSNTD is based on the following principle: when an ionising particle passes through insulating solids, it creates narrow paths of intense damage on an atomic scale [1]. These damages can be revealed and made visible in an ordinary optical microscope, by treatment with a properly chosen chemical reagent. By the chemical treatment the undamaged material of the detector is etched with a constant velocity  $v_{\text{B}}$  and the damaged regions with a velocity  $v_{\text{T}}$ , where  $v_{\text{T}} > v_{\text{B}}$ . As a result, an etched cone (nuclear track) is formed, which is visible by an optical microscope. What we see in this case is the intersection of the etched cone with the detector surface, which in most cases is a dark ellipse on brighter background.

The track velocity  $v_{\text{T}}$  is a function of the Restricted Energy Loss (REL) which is defined as the part of the Energy Loss including only ionisations in which  $\delta$ -electrons with an energy below a threshold  $w_0$  are generated. In CR-39 (which is the type of SSNTD we used)  $w_0$  is determined to be 200 eV [2].

Somogyi [3] has derived the relation between track velocity ( $v_T$ ) and the radius of a circular track ( $R$ ):

$$v_T = v_B \frac{(v_B t)^2 + R}{(v_B t)^2 - R} \quad (1)$$

here  $t$  is the etching time and  $v_B$  the bulk velocity of the detector.

Since  $v_T = f_1(\text{REL})$  and  $\text{REL} = f_2(Z, E)$ ,  $v_T = f_3(Z, E)$  and equivalently  $R = f(Z, E)$  since the relation between  $R$  and  $v_T$  is well known. For energies above 800 MeV/n, REL remains approximately constant, therefore  $R$  is a function of  $Z$  only [4].

The experimental set up for measuring the projectile fragmentation cross sections is shown in Fig 1. A stack of three CR-39 foils is placed in front of the target (upstream) in order to register the incoming beam particles, and another stack of three CR-39 foils is placed after the target (downstream) in order to identify the outgoing beam particles and projectile fragments.

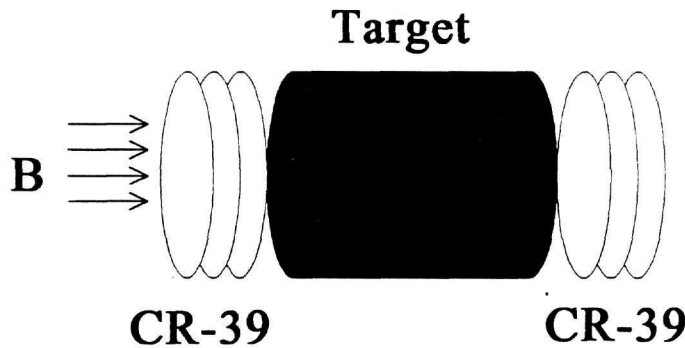


Figure 1. Experimental setup

## 2. Image Analysis System

For scanning the detector surfaces and measuring the track radii we used an automatic measuring system which has been developed based on image analysis techniques [5]. The principal components of the system are a PC-486 computer with a frame grabber, an image display monitor, an optical microscope on which a motorised stage has been adjusted and a video camera (Fig. 2). The software for the image analysis and track recognition has been entirely developed in order to fulfil the requirements of automatic measurements.

Each detector foil is mounted on the microscope stage which can be moved by stepping motors under the control of the computer. The image of the microscope is taken by the video camera and digitized by the frame grabber to a 512x512 pixels digital image. The nuclear tracks which appear as dark areas are recognised by the software. For

each track the parameters that are determined are the radius, the center coordinates and the brightness in the center of the track.

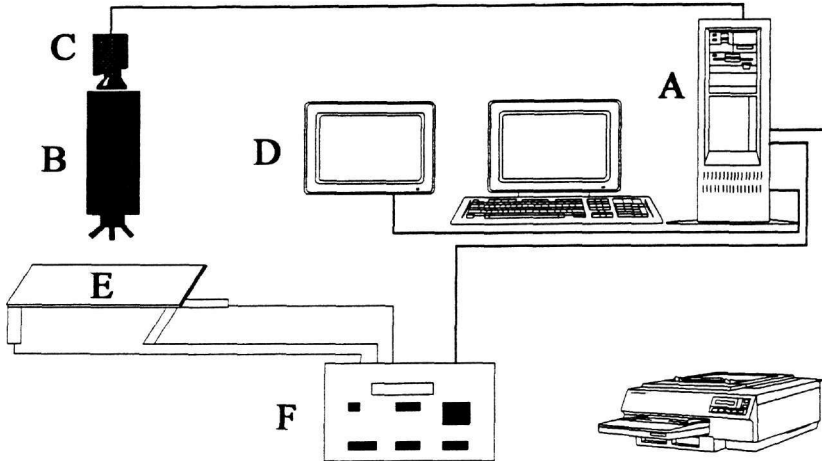


**Figure 2.** The principal components of the Image Analysis System: A PC-486 computer with a frame grabber, B optical microscope, C video camera, D image display monitor, E motorised stage, F stage controller

## 2. Experimental Results

Tracks were measured, upstream and downstream Pb, Cu and Al targets, using the image analysis system. The results from the Pb target (downstream) are shown in Fig 3. The two pronounced peaks are due to  $^{16}\text{O}$  and  $^{32}\text{S}$  beam particles which came out of the target without having interacted with it. No other peaks due to intermediate charge fragments ( $8 < Z < 16$ ) produced by projectile fragmentation are easily distinguished.

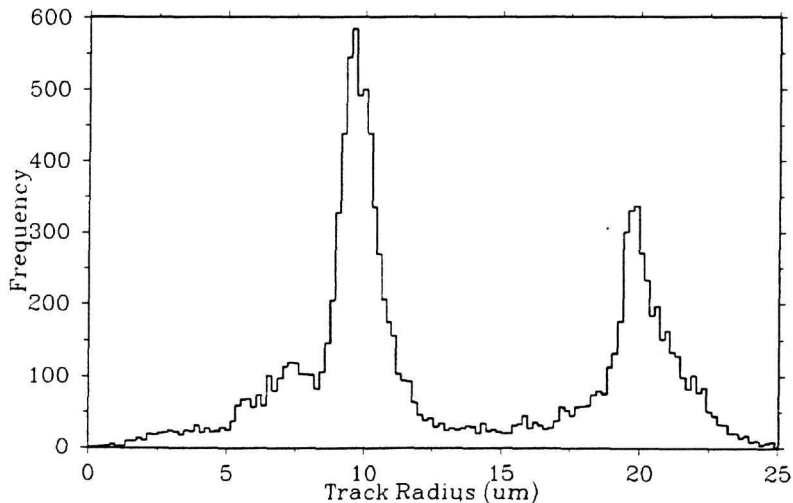


**Figure 3.** Track radii distribution from the Pb target (downstream)

The measurements are further processed in order to

- i) reject tracks due to detector background,
- ii) correct track radii due to microscope inhomogeneous illumination.

The data presented in Fig. 3 after the processing are shown in Fig 4. Intermediate peaks are now clearly distinguished for each fragment charge from  $Z=7$  to  $Z=16$ .

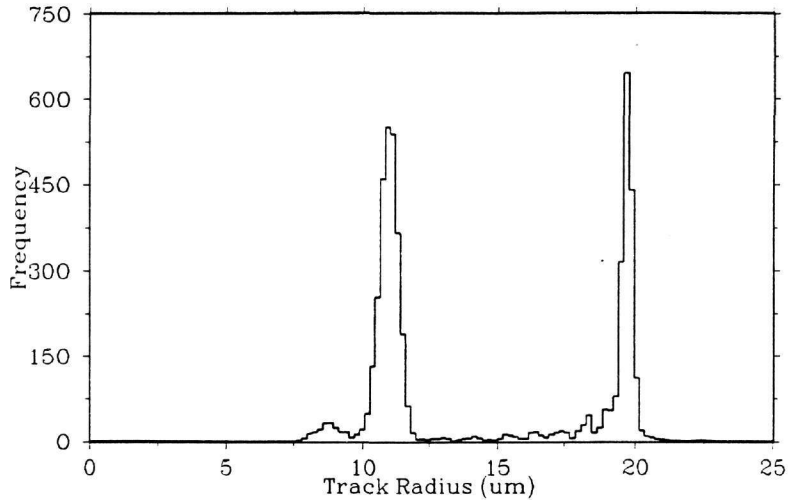


**Figure 4.** Track radii distribution from the Pb target (downstream) after data processing

A numerical fitting method using successive minimisations has been used, in order to fit our results, with ten gaussian peaks, corresponding to each fragment charge from  $Z=7$  to  $Z=16$ . The linear relationship between track radius and the position of each peak is dictated by the linear relationship between track radius  $R$  and particle charge  $Z$ .

Table 1. shows the number of tracks measured upstream and downstream the Cu, Ag and Pb targets, for each charge fragment.

#### 4. Total and Partial cross sections

From the number of tracks measured for each charge  $Z$ , upstream and downstream the target the total and partial cross sections can be calculated using the following formula [6]:

$$N_i(x) = N_i(0)e^{-x\sigma_i} + \sum_{j=1}^{i-1} k_{ij}(e^{-x\sigma_j} - e^{-x\sigma_i}) \quad (2)$$

$$k_{ij} = \frac{1}{\sigma_i - \sigma_j} \left\{ \sigma_j N_j(0) - \sum_{n=j+1}^{i-1} \sigma_n k_{nj} + \sum_{n=1}^{j-1} \sigma_n k_{jn} \right\}$$

where  $x$  transformed depth in target  $x = N_A \rho t / A$ ,  $N_A$  Avogadro's number,  $\rho$  target density,  $A$  target atomic number,  $t$  depth in the target,  $N_i(0)$  number of tracks of charge  $Z_i$  at  $x=0$ , where  $Z_1=16$  and  $Z_{10}=7$ ,  $N_i(x)$  same at arbitrary  $x$ ,  $\sigma_i$  total charge changing cross section of nucleus with charge  $Z_i$  in the target,  $\sigma_{ij}$  cross section of the production of a projectile fragment of charge  $Z_i$  in a collision of a projectile nucleus of charge  $Z_j$  on the target.

Fragment charge	Target					
	Cu		Ag		Pb	
	Up	Down	Up	Down	Up	Down
7	323	372	317	382	214	190
8	4527	3476	4257	3022	3837	2638
9	14	22	15	30	15	26
10	12	29	12	36	16	29
11	8	35	13	43	9	41
12	10	45	19	50	13	46
13	27	42	10	36	18	78
14	41	100	64	115	56	100
15	31	106	33	106	31	138
16	2997	1992	2912	1721	2860	1595

**Table 1.** Number of tracks measured upstream and downstream the Cu, Ag and Pb targets

Table 2 shows the total charge changing cross sections for  $^{32}\text{S}$  and  $^{16}\text{O}$  at 3.65 GeV/n for the Cu, Ag and Pb targets, as well as the partial cross sections for production of fragments with charge  $8 < Z < 16$ , calculated using the formula (2).

The results are compared with theoretical values according to Geometrical and Soft-spheres models. According to the Geometrical model [7], the nucleus-nucleus cross section is given by the formula

$$\sigma_G = \pi r_0^2 (A_T^{1/3} + A_P^{1/3} - b)^2 \quad (3)$$

where  $A_T$  and  $A_P$  are the target and projectile mass, respectively, and  $r_0$  and  $b$  are parameters. According to Soft-spheres [8] model the total nucleus-nucleus cross section

can be expressed by the geometrical formula in which the overlap parameter  $b$  is given by Vary's relation

$$b = b_0 (A_T^{1/3} + A_P^{1/3})^2 \quad (4)$$

where  $b_0$  is the curvature correction parameter.

Charge	Target					
	Cu		Ag		Pb	
	$\sigma_{tot}$	$\sigma_{nl}$	$\sigma_{tot}$	$\sigma_{nl}$	$\sigma_{tot}$	$\sigma_{nl}$
8	1741±59		1950±65		2986±75	
9		46±3		76±4		81±5
10		70±4		103±5		89±5
11		92±4		116±5		178±7
12		133±6		129±6		187±7
13		122±6		115±6		308±8
14		261±8		234±8		326±9
15		307±9		315±9		637±10
16	2691±95		2994±87		4653±93	

**Table 2.** Total and partial cross sections (in mb) for  $^{32}\text{S}$  and  $^{16}\text{O}$  at 3.65 GeV/n for the Cu, Ag and Pb targets.

Table 3 shows the comparison of the total reaction cross sections (in mb) for  $^{32}\text{S}$  and  $^{16}\text{O}$  determined in the present experiment with the calculated values according to Geometrical model, Soft-spheres model and other experiments. For the Geometrical model parameters have been taken as  $r_0=1.2$  fm and  $b=1.32$ . For the Soft-spheres model parameters have been taken as  $r_0=1.37$  fm and  $b_0=0.75$ .

beam	target	this work	Geometrical Model	Soft-spheres Model	Ref. 9	Ref. 10
32S	Cu	2691±95	1551	2796		2428±61
	Ag	2994±87	1981	3468		3043±83
	Pb	4653±93	2731	4611		8560±110
16O	Cu	1741±59	1223	2259	1950±41	
	Ag	1950±65	1608	2867		
	Pb	2986±75	2290	3913	3270±82	

**Table 3.** Comparison of the total reaction cross sections (in mb) for  $^{32}\text{S}$  and  $^{16}\text{O}$  determined in the present experiment with Geometrical model, Soft-spheres model and other experiments.

The data from Lindstrom P.G. et al. [Ref 9], correspond to 2.1 GeV/n. The data from Brechtman C. and Heinrich W. [Ref 10] correspond to 1.2 GeV/n for Cu target, to 0.7 GeV/n for Ag target and to 60 GeV/n for Pb target. Our results are compatible with cross sections deduced from soft spheres model than to geometrical model.

### 5. Conclusions

The experimental technique of computerized track measurements in CR-39 solid state track detector offers the possibility of collecting a large number of data with very good charge resolution. The experiment objective was to determine the cross sections of several reactions and the discrimination fragment charges produced by projectile fragmentation.

### References

- [1] Fleischer R.L., Price P.B. and Walker, Nuclear Tracks in Solids, University of California Press, Berkeley 1975.
- [2] D.L.Henshaw et. al. Nucl.Instr. and Methods 180, 65, (1981).
- [3] G.Somogyi and S.A.Szalay, Nucl.Instr. and Methods 109, 211 (1973).
- [4] J.Dreute et.al. Phys.Rev.C 44,3 (1991) 1057.
- [5] D.Sampsonidis and M.Zamani, Microprocessing and Microprogramming 34 (1992) 153.
- [6] Brechtmann C. and Heinrich W., Nucl.Instr. and Methods B29 (1988) 675.
- [7] Bradt H.C. and Peters B., Phys.Rev 77, (1950) 54.
- [8] Karol P.J. Phys.Rev.C 11 (1975) 1203.
- [9] Lindstrom P.G. et. al., Bull.Am.Phys.Soc. 17 (1972) 488.
- [10] Brechtmann C. and Heinrich W., Z.Phys. A331 (1988) 463.